Available online at www.sciencedirect.com

ScienceDirect

Nuclear and Particle Physics Proceedings 267–269 (2015) 345–352

www.elsevier.com/locate/nppp

Systematic uncertainties from halo asphericity in dark matter searches

Nicolás Bernal[a], Jaime E. Forero-Romero[b], Raghuveer Garani[c], Sergio Palomares-Ruiz[d]

[a]*ICTP South American Institute for Fundamental Research and Instituto de Física Teórica, Universidade Estadual Paulista, São Paulo, Brazil*
[b]*Departamento de Física, Universidad de los Andes, Cra. 1 No. 18A-10, Edificio Ip, Bogotá, Colombia*
[c]*Bethe Center for Theoretical Physics and Physikalisches Institut, Universität Bonn, Nußallee 12, D-53115 Bonn, Germany*
[d]*Instituto de Física Corpuscular (IFIC), CSIC-Universitat de València, Apartado de Correos 22085, E-46071 València, Spain*

Abstract

Dark matter halos are predicted to be non-spherical by N-body simulations. Using data from the large N-body cosmological simulation `Bolshoi`, we quantify the systematic uncertainties due to halo asphericity on the determination of local dark matter density and the *J* factors for dark matter annihilations and decay from the galactic center.

Keywords: Dark matter, N-body Simulations, triaxial halos.

1. Introduction

The existence of non-luminous Dark Matter (DM) is by now well established [1, 2]. In order to detect and constrain the nature of DM three complementary and competing strategies have been developed, namely: collider searches, direct and indirect searches. In contrast to collider DM searches, direct and indirect methods depend crucially on the properties of the Milky Way DM halo. For example: direct detection experiments depend on the flux of halo DM particles streaming through the detector, which naturally depends on the local density of DM particles. Indirect detection experiments which measure the flux of gamma-rays and neutrinos that are products of DM annihilations or decays, depend on the shape and orientation of DM halo in the direction of observation.

The Milky Way is usually modeled by decomposing the galaxy into three components: the bulge, the disc and the dark halo respectively; with the bulge and the disc embedded in a spherical DM halo. However, it is well known that N-body simulations of structure formation predict DM halos to be triaxial. In this talk we revisit the question: "What is the impact of halo asphericity on direct and indirect searches?" [1]. To formulate a sensible answer we analyze a sample of 10^5 DM-only Milky Way like halos from Bolshoi simulation [5].

The remainder of the talk (based on Ref. [6]) is organized as follows: In Sec. 2 we emphasize the dependence of direct and indirect methods on DM halo density profile. The data we select from the Bolshoi simulation to construct the density profile is briefly discussed in Sec. 3. In Sec. 4 we use three examples to illustrate the impact of halo asphericity on the local DM density and on the so-called *J* factors. Sec. 5 is devoted to the observational priors used. The conclusions are presented in the last section.

2. Direct and Indirect Searches

Direct detection experiments aim at detecting halo DM particles by measuring nuclear recoils resulting from scattering of DM with the nuclei in the detector. Qualitatively, the event rate *R* is given by [7]

Email addresses: `nicolas@ift.unesp.br` (Nicolás Bernal), `je.forero@uniandes.edu.co` (Jaime E. Forero-Romero), `garani@th.physik.uni-bonn.de` (Raghuveer Garani), `sergio.palomares.ruiz@ific.uv.es` (Sergio Palomares-Ruiz)

http://dx.doi.org/10.1016/j.nuclphysbps.2015.10.129

[1] The effects of triaxiality on the estimates for the local DM density have been studied in Ref. [3], using a simulation with only DM, and in Ref. [4], with simulations of two Milky-Way-like galaxies including baryons.

$$R \approx \frac{\rho_\odot \, \sigma \, \langle v \rangle}{m_\chi \, m_A} \, . \tag{1}$$

Here σ is the DM-nuclei scattering cross section, $\rho_\odot$ is the local DM density, $\langle v \rangle$ is the average relative speed of DM with respect to the target, m_χ is the DM mass and m_A is the mass of the target nuclei. Thus, the measurement of recoil rate is directly proportional to the local DM density, $\rho_\odot$.

For indirect detection of DM annihilations or decays from the galactic center (GC), the spatial distribution of DM in the halo is important. The differential flux of resultant products (prompt gamma-ray or neutrinos) of DM annihilation (decays) in the smooth Milky Way DM halo coming from a direction within a solid angle $\Delta\Omega$, can be written as [8]

$$\begin{aligned} \frac{d\Phi_{\rm ann}}{dE}(E, \Delta\Omega) &= \frac{\langle \sigma v \rangle}{2\, m_\chi^2} \sum_i {\rm BR}_i \, \frac{dN^i_{\rm ann}}{dE} \, \bar{J}_{\rm ann}(\Omega) \, \frac{\Delta\Omega}{4\,\pi} \, , \\ \frac{d\Phi_{\rm dec}}{dE}(E, \Delta\Omega) &= \frac{1}{m_\chi \, \tau_\chi} \sum_i {\rm BR}_i \, \frac{dN^i_{\rm dec}}{dE} \, \bar{J}_{\rm dec}(\Omega) \, \frac{\Delta\Omega}{4\,\pi} \, . \end{aligned} \tag{2}$$

Here $\langle \sigma v \rangle$ is the thermally averaged total DM annihilation cross section times the relative velocity, τ_χ is the DM lifetime, the discrete sum is over all DM annihilation (decay) channels, ${\rm BR}_i$ is the branching ratio of DM annihilation (decay) into the i-th final state and $dN^i_{\rm ann}/dE$ ($dN^i_{\rm dec}/dE$) is the differential gamma-ray or neutrino spectrum from the i-th channel. The quantities $\bar{J}_{\rm ann}(\Omega)$ and $\bar{J}_{\rm dec}(\Omega)$, also known as J-factors, which depend on the DM distribution are defined as

$$\begin{aligned} \bar{J}_{\rm ann}(\Omega) &= \frac{1}{\Delta\Omega} \int_{\Delta\Omega} {\rm d}\Omega \int_{\rm los} \rho(r(s,\Omega))^2 \, {\rm d}s \, , \\ \bar{J}_{\rm dec}(\Omega) &= \frac{1}{\Delta\Omega} \int_{\Delta\Omega} {\rm d}\Omega \int_{\rm los} \rho(r(s,\Omega)) \, {\rm d}s \, . \end{aligned} \tag{3}$$

Here the integral of $\rho(r)^2$ and $\rho(r)$ is performed along the line of sight within the solid angle of observation $\Delta\Omega$.

3. Bolshoi Simulation

The data used in this work is publicly available through the *MultiDark Database*[2] presented in Ref. [9]. The cosmological parameters, which are inputs to the simulation, are compatible with the results from the ninth year data releases from the Wilkinson Microwave Anisotropy Probe [10], with $\Omega_m = 0.27$, $\Omega_\Lambda = 0.73$, $n_s = 0.95$, $h = 0.70$ and $\sigma_8 = 0.82$ for the matter density, dark energy density, slope of the matter fluctuations, the Hubble parameter at $z = 0$ in units of 100 km s^{-1} Mpc^{-1} and the normalization of the power spectrum, respectively. With these parameters the mass of a simulation particle is $m_p = 1.4 \times 10^8 h^{-1} {\rm M}_\odot$. The simulation follows the non-linear evolution of DM density fluctuations in a cube of length $250 h^{-1}$ Mpc with 2048^3 particles. The halos formed in this simulation are well fit by Navarro-Frenk-White (NFW) profile [11, 12].

The data set we analyze contains 87132 halos which have virial masses in the Milky Way range, i.e., $M_v = [0.7, 4.0] \times 10^{12} \, {\rm M}_\odot$. Typically a spherically symmetric DM density profile can be parametrized by two variables, the virial mass M_v and concentration parameter c_a. However, in order to describe a triaxial halo two more variables are required which describe the shape: the axes ratios b/a and c/a. Here $a \geq b \geq c$ are the eigenvalues of the shape tensor for a given halo.

The standard spherically symmetric NFW profile is given by

$$\rho(r) = \frac{N}{(r/r_s)\,[1 + (r/r_s)]^2} \, , \tag{4}$$

and is generalized to a triaxial shape by re-parameterizing r as,

$$r \to r_e = \sqrt{x^2 + \left(\frac{y}{b/a}\right)^2 + \left(\frac{z}{c/a}\right)^2} \, .$$

The resulting distributions for the parameters of triaxial NFW profile are shown with the black lines in Fig. 1. The average values of the parameters in this sample are: $\langle M_v \rangle = 1.55 \times 10^{12} \, {\rm M}_\odot$, $\langle c_e \rangle = 8.9$, $\langle b/a \rangle = 0.81$ and $\langle c/a \rangle = 0.66$.

Hierarchical structure formation predicts that massive halos are formed by mergers of smaller halos. This feature is nicely illustrated in the probability distribution of M_v in Fig. 1. A larger number of halos exist for low masses. This dependence of the halo abundance as a function of halo mass is well understood and is parametrized through the halo mass function. However, as for the Milky Way, its mass is quite uncertain (within an order of magnitude). In order to avoid an unfair weight to the low mass range due to cosmological effects in the simulation, we also consider a flat prior on M_v by weighting all bins such that all values of M_v, in the range $M_v = [0.7, 4.0] \times 10^{12} \, {\rm M}_\odot$, are equiprobable. With this exercise we can study systematic effects

[2] http://www.multidark.org/MultiDark/MyDB

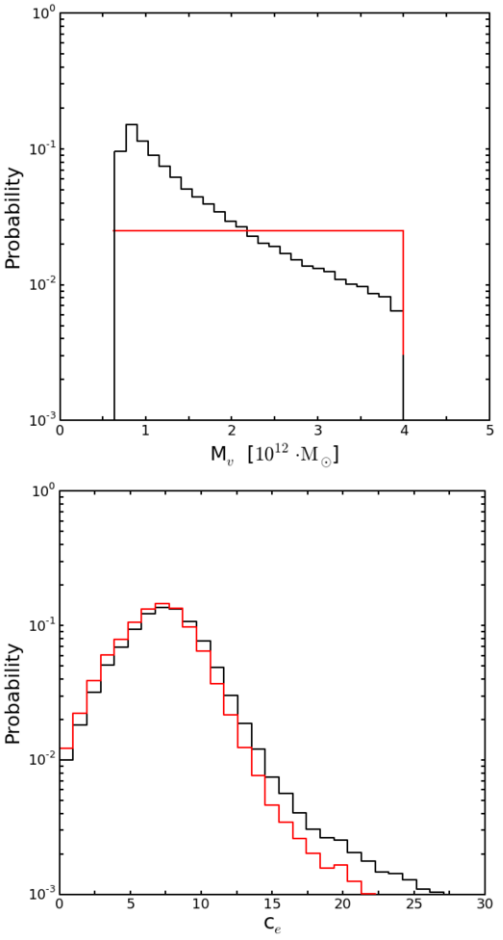

Figure 1: ***Probability distributions of the halo parameters***: black lines for our data sample and red lines when a flat prior on M_v is imposed. The upper panel depicts the probability distributions of the halo mass M_v and the lower panel the probability distributions of the concentration parameter c_a.

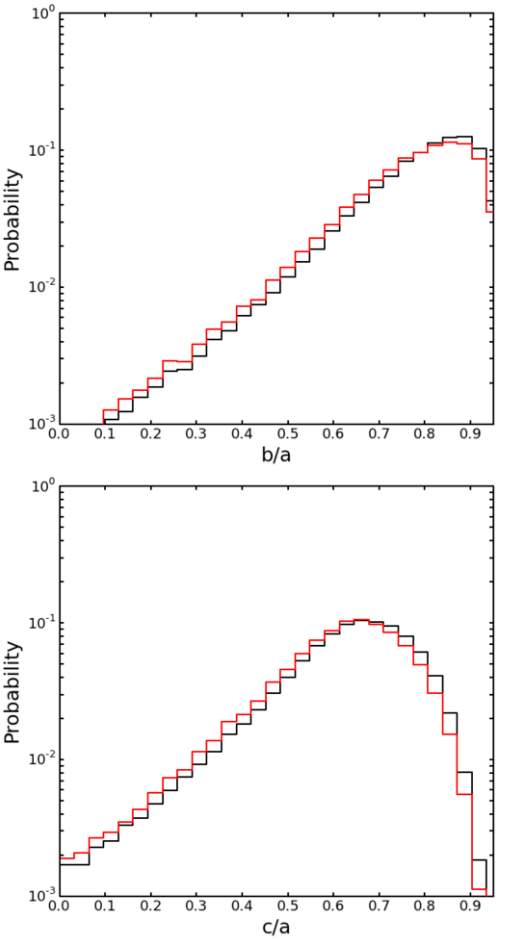

Figure 2: ***Probability distributions of the halo parameters***: black lines for our data sample and red lines when a flat prior on M_v is imposed. The upper panel depict the probability distributions of the axes ratio b/a and the lower panel depict probability distributions of the axes ratio c/a.

independently of the cosmological bias. The probability distributions of the parameters for this re-weighted sample, with a flat prior on the halo mass, are depicted in Figs. 1 and 2 with the red curves.

4. Impact of Halo Asphericity

In this section we describe the possible impact of having a non-spherical halo on quantities such as the local DM density ($\rho_\odot$) and J factors. Consider a set of observers at a given distance from the halo center who are able to locally measure properties of the halo and are able to compute $\rho_\odot$. In a spherically symmetric halo all observers would obtain the same value. However, in a triaxial halo these measurements would lead to a significant variance with respect to the spherically averaged value [13]. We show that there exists similar deviations from the spherically averaged value for J factors as well.

We consider three example halos: an almost spherical halo ($a \approx b \approx c$) , a prolate halo ($a \gg b \approx c$) and an oblate halo ($a \approx b \gg c$). We assume the galactic disc to coincide with one of the symmetry planes of the dark halo. Consequently, our ignorance of where the solar system might reside in a triaxial halo motivates us to evaluate the aforementioned quantities individually for each plane of symmetry.

With the halo profile exactly defined by M_v, c_e, b/a and c/a, we proceed to compute the local DM density, $\rho_\odot$, and the J factors for a region of interest (ROI) of

$3^\circ \times 3^\circ$ (a square of 3° side) around the GC. We do so for different points along a circle of radius ($R_\odot \approx 8.3$ kpc) for the three planes of symmetry. Then, we compute the average quantities in a spherical shell of the same radius[3], $\langle \rho_\odot \rangle$. The results corresponding the approximately spherical halo are depicted in Fig. 3; where we show the deviation of $\rho_\odot$ with respect to its spherical average as a function of the angular position θ along a circle of radius $R_\odot$. We choose $\theta = 0$ as a reference point, which corresponds to the occurrence of the maximum value of each quantity. In all panels, the solid red, dashed blue and dotted black curves indicate the variation along the $a-b$ plane, the $a-c$ plane and the $b-c$ plane, respectively. Similar results are found for $\langle \bar{J}_{\rm ann} \rangle$ and $\langle \bar{J}_{\rm dec} \rangle$ [6].

As expected, the deviations from the spherical average are the smallest for the approximately spherical halo. A maximum variation of $\sim 5\%$ for the local DM density is found and only $\sim 1.6\%$ and $\sim 2.5\%$ for $\bar{J}_{\rm ann}$ and $\bar{J}_{\rm dec}$, respectively. On the other hand, in the case of the prolate halo we consider here, deviations of up to $\sim 46\%$, $\sim 14\%$ and $\sim 20\%$ are possible for $\rho_\odot$, $\bar{J}_{\rm ann}$ and $\bar{J}_{\rm dec}$, respectively. The oblate halo considered here being closer to the spherical case, presents deviations of up to $\sim 20\%$, $\sim 6\%$ and $\sim 9\%$ for $\rho_\odot$, $\bar{J}_{\rm ann}$ and $\bar{J}_{\rm dec}$, respectively.

Its important to note that the deviations for the J factors are larger for DM decay than for DM annihilation. Heuristically, this can be understood by considering the contributions to the J factors away from the center of the halo for a given ROI. For DM annihilations, the relative contribution to the J factors from the outer regions (i.e., regions which are closer to the boundary of the ROI) with respect to the contribution from the center is expected to be smaller than for DM decays. Hence, the deviations from the spherical average are smaller for DM annihilations. We encounter this below once again when discussing our results.

Thus halo asphericity could give rise to significant deviations from the spherically averaged values of relevant quantities for DM searches. Indeed, these deviations could be quite large depending on the shape of the halo and could have a substantial impact on direct and indirect DM detection. In the following, we quantify these uncertainties statistically by using the whole halo data set.

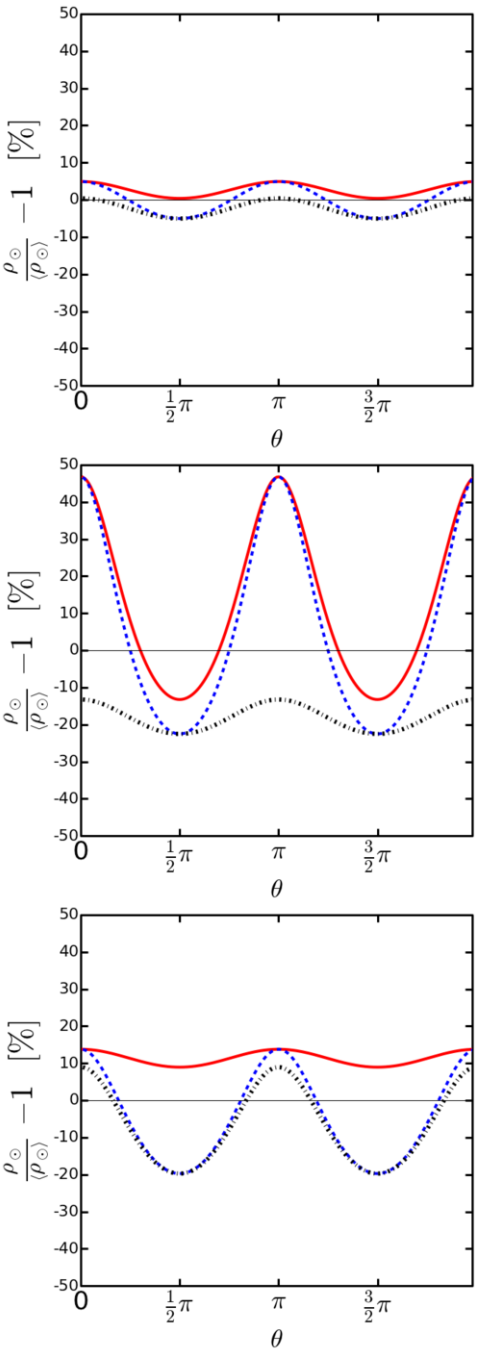

Figure 3: ***Deviation from the average DM local density in a spherical shell of radius $R_\odot$ for the three symmetry axes.*** The results shown are for the following DM halos: approximately spherical (upper panel), prolate (middle panel) and oblate (lower panel). The $a-b$ plane is represented by the solid red curve, the $a-c$ plane by the dashed blue curve and the $b-c$ plane by the dotted black curve. The angle θ represents the angular position along a circle of radius $R_\odot$ for each plane of symmetry.

[3]The average density $\langle \rho_\odot \rangle$ is the quantity inferred from dynamical measurements in the galaxy.

	Gaussian priors	
	Central value	1σ error
$M_{60}^{\rm DM}$ [$10^{11}\,{\rm M}_\odot$]	$M_{60}^{\rm DM} = 4.0$	$\sigma_{60} = 0.7$
$\Sigma_{1.1}^{\rm DM}$ [${\rm M}_\odot\,{\rm pc}^{-2}$]	$\Sigma_{1.1}^{\rm DM} = 17$	$\sigma_\Sigma = 6$

Table 1: Limits for the central values and 1σ errors for the enclosed DM halo mass at 60 kpc ($M_{60}^{\rm DM}$) [14] and the local DM surface density ($\Sigma_{1.1}^{\rm DM}$) [15], which are used for the priors discussed in the text.

	Flat priors	
	Lower cut	Upper cut
M_v [$10^{12}\,{\rm M}_\odot$]	$M_v^{\rm min} = 0.7$	$M_v^{\rm max} = 4.0$
$R_\odot$ [kpc]	$R_\odot^{\rm min} = 7.5$	$R_\odot^{\rm max} = 9$

Table 2: Limits for the halo virial mass (M_v) and the Sun's galactocentric distance ($R_\odot$), which are used for the priors discussed in the text.

5. Observational Priors

To realistically estimate the systematic effects due to the halo shape we include several observational constraints as priors in our analysis. In addition to a flat prior on the virial mass, we also include Gaussian priors on the enclosed mass at 60 kpc, the local DM surface density and the Sun's galactocentric distance. Hence, for each plane of symmetry, the probability distribution function of the original data sample is modified as:

$$\begin{aligned}{\rm PDF}^p_{\rm prior}(\vec{\omega}) =& C\frac{{\rm PDF}(\vec{\omega})}{{\rm PDF}(M_v)} \times \theta(M_v - M_v^{\rm min})\,\theta(M_v^{\rm max} - M_v) \\ &\times \int_{{\rm R}_\odot{}^{\rm min}}^{{\rm R}_\odot{}^{\rm max}} {\rm dR}_\odot \exp\left[-\frac{(M_{60}^{\rm DM} - M_{60})^2}{2\,\sigma_{60}^2}\right] \\ &\times \int_0^{2\pi} {\rm d}\psi\, \exp\left[-\frac{(\Sigma_{1.1}^{\rm DM} - \Sigma_{1.1}^p({\rm R}_\odot,\psi))^2}{2\,\sigma_\Sigma^2}\right],\end{aligned} \tag{5}$$

where C is a normalizing constant, $\vec{\omega} = (M_v,\, c_e,\, b/a,\, c/a)$, ${\rm PDF}(\vec{\omega})$ is the original probability distribution function and ${\rm PDF}(M_v)$ is the probability distribution function after marginalizing over $(c_e, b/a, c/a)$. ${\rm PDF}^p_{\rm prior}(\vec{\omega})$ is computed for the three symmetry planes, $p = a-b$, $a-c$ and $b-c$, where ψ is the azimuthal angle at the solar circle. The limits, central values and errors, are indicated in Tab. 1 and Tab. 2 for Gaussian and flat priors respectively. Note that the prior on M_{60} is a global prior for a given halo, whereas the prior on the DM surface density is a local constraint which depends on the exact position of the observer in the halo and thus, on the plane of symmetry under consideration [6].

6. Results

Using an ellipsoidal NFW profile for each halo in the simulation sample, we evaluate the probability distribution of variations with respect to the spherically averaged quantities of interest in this work: the local DM density and the so-called J factors in indirect DM searches.

All halos are binned according to their value of the spherical average $\langle O\rangle$. Here O is an observable equal to $\rho_\odot$ or $\bar{J}_{\rm ann}$ or $\bar{J}_{\rm dec}$, depending on the context. Then, for every halo, O is evaluated in a grid of 300 different points along a circle of radius $\rm R_\odot$ for each plane of symmetry and for 6 values of $\rm R_\odot$ covering the range in Tab. 2. The results for the deviations from the spherically averaged value are depicted in Figs. 4, 5 and 6, corresponding to $\rho_\odot$, $\bar{J}_{\rm ann}$ and $\bar{J}_{\rm dec}$ respectively. In the figures, we show the deviation of O from its spherically averaged value $\langle O\rangle$ for the three symmetry planes as a function of $\langle O\rangle$. The dark blue (light orange) contours represent the 68% (95%) most probable regions of the deviation. On the top and the right of each panel the projected probability distributions of $\langle O\rangle$ and $\frac{O}{\langle O\rangle} - 1$ are depicted, respectively.

6.1. Systematic uncertainties on $\rho_\odot$

The value of $\rho_\odot$ deduced from most dynamic measurements often refers to the spherically averaged density $\langle\rho_\odot\rangle$. We noted that, in a non-spherical halo, the actual DM density in the solar neighborhood could actually differ significantly from that value (see Sec. 4). Here, we consider the whole sample of halos and study this type of uncertainties as a function of the local average of the DM density.

In the principal plane $a-b$, the local density tends to adopt values larger than those of the average density, whereas in the plane $b-c$ the values are typically smaller than the average. The deviations (in absolute value) in the $a-b$ plane are larger compared to the ones in the $b-c$ plane due to the fact that there are more prolate than oblate halos. The densities in the plane $a-c$ are intermediate, spanning over a large range that goes from the lowest values reached in the $b-c$ plane to the highest values in the $a-b$ plane.

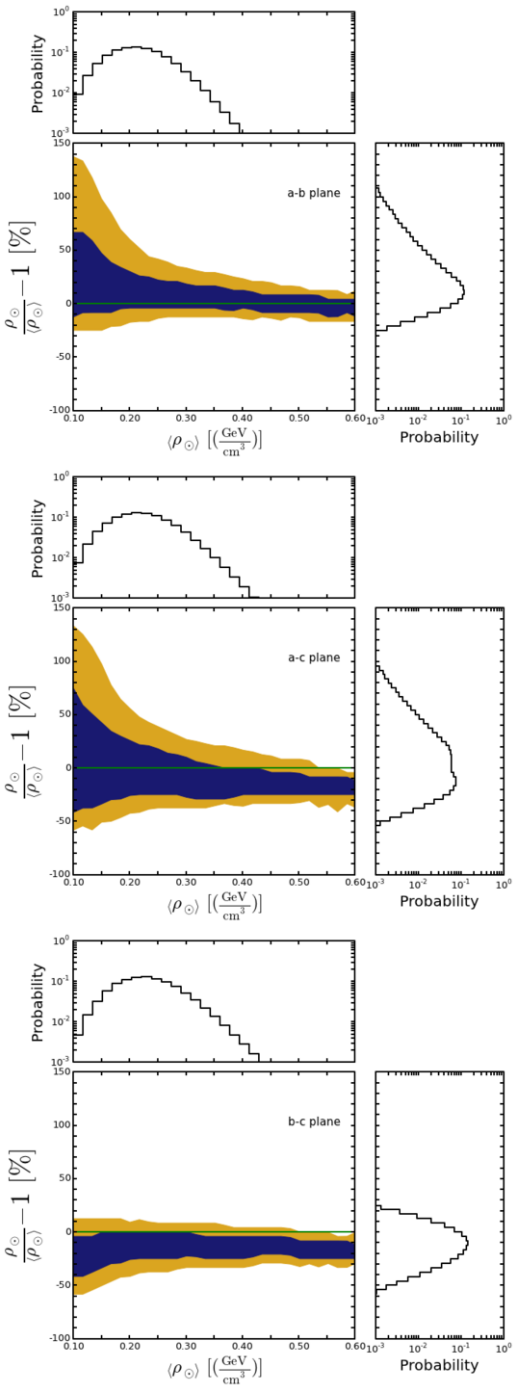

Figure 4: ***Systematic uncertainties on $\rho_\odot$, due to the non-sphericity of the Milky Way DM halo.*** We depict the probability distribution of the deviation of the local DM density from its spherically average value, $\langle\rho_\odot\rangle$, for the three symmetry planes as a function of $\langle\rho_\odot\rangle$. The dark blue (light orange) contours represent the 68% (95%) most probable regions. On the top and the right of each panel we depict the projected probability distribution with respect to that quantity.

Fig. 4 shows important deviations with respect to the spherically averaged local DM density, especially for low values, $\langle\rho_\odot\rangle \lesssim 0.2$ GeV/cm^3. Such small values for $\langle\rho_\odot\rangle$ are common in very triaxial halos which, in turn, naturally generate large deviations. We also note that the deviations are of the order of $^{+20\%}_{-5\%}$ $\left(^{+40\%}_{-15\%}\right)$, $^{+15\%}_{-30\%}$ $\left(^{+35\%}_{-40\%}\right)$ and $^{+0\%}_{-30\%}$ $\left(^{+10\%}_{-35\%}\right)$ for the 68% (95%) most probable regions in the $a-b$, $a-c$ and $b-c$ planes, respectively.

6.2. *Systematic uncertainties on $\bar{J}_{\rm ann}$ and $\bar{J}_{\rm dec}$*

Analogous to the analysis performed to estimate the uncertainties on the local DM density (Fig. 4), we compute the systematic uncertainties, caused by the non-sphericity of the Milky Way DM halo, on the determination of the J factors for DM annihilation and decay. Our results are depicted in Fig. 5 for $\bar{J}_{\rm ann}$ and in Fig. 6 for $\bar{J}_{\rm dec}$, as a function of their spherically averages, $\langle\bar{J}_{\rm ann}\rangle$ and $\langle\bar{J}_{\rm dec}\rangle$, for the three symmetry planes and for a square ROI of $3^\circ \times 3^\circ$ around the GC. These figures have essentially the same features of Fig. 4: for intermediate and high values of $\langle\bar{J}\rangle$, approximately the same uncertainty is found, whereas larger errors are obtained for low values[4] of $\langle\bar{J}\rangle$. For DM annihilations (Fig. 5) and for intermediate and high values of $\langle\bar{J}_{\rm ann}\rangle$, the deviations are of the order of a few percent (up to $\sim$10%) for the 68% (95%) most probable regions. On the other hand, for DM decays (Fig. 6), the deviations from the average value for intermediate and high $\langle\bar{J}_{\rm dec}\rangle$, are of the order of a few percent, up to $\sim$10% (up to $\sim$15%) for the 68% (95%) most probable regions. Finally, let us stress that we have verified that the variations with respect to the average value for the J factors depend very weakly on the chosen ROI.

7. Discussion and summary

Using data from large N-body simulation `Bolshoi` we have presented the probability distributions of the parameters that define their shape and use them to study the impact of halo asphericity on the determination of the local DM density and the J factors relevant for indirect searches of signals from the GC. This is illustrated in Sec. 4 with three example halos: an approximately spherical halo, a prolate halo and an oblate halo.

[4]The bump in Fig. 6, which occurs at very low values of $\langle\bar{J}_{\rm dec}\rangle$, is due to the presence of a small number of approximately spherical halos with very large concentrations in the first bin, which further get favorably weighted by the priors. It is a statistical effect due to the finite size of the sample and the chosen size of the bins. It does not show up in Fig. 5 because the number of halos in the first bin is two orders of magnitude larger.

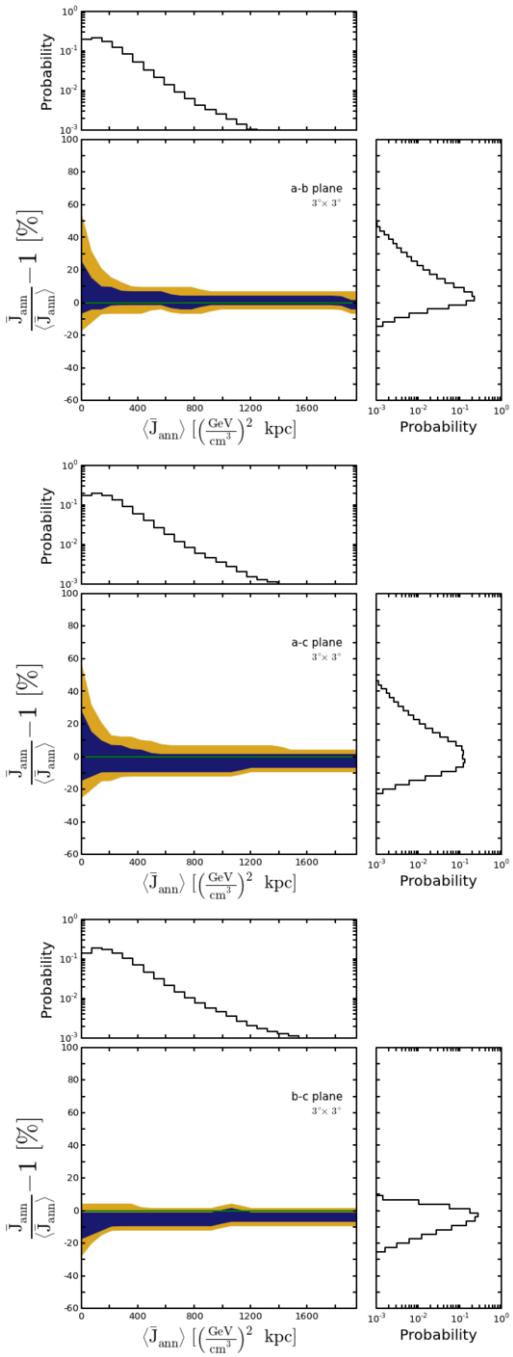

Figure 5: ***Systematic uncertainties on $\bar{J}_{\rm ann}$ for a square ROI of 3° × 3° around the GC for DM annihilations, due the non-sphericity of the Milky Way DM halo.*** We show the probability distribution of the deviation of $\bar{J}_{\rm ann}$ from its spherically average value, $\langle\bar{J}_{\rm ann}\rangle$, for the three symmetry planes as a function of $\langle\bar{J}_{\rm ann}\rangle$. The panels and colors of the different contours represent the same as in Fig. 4.

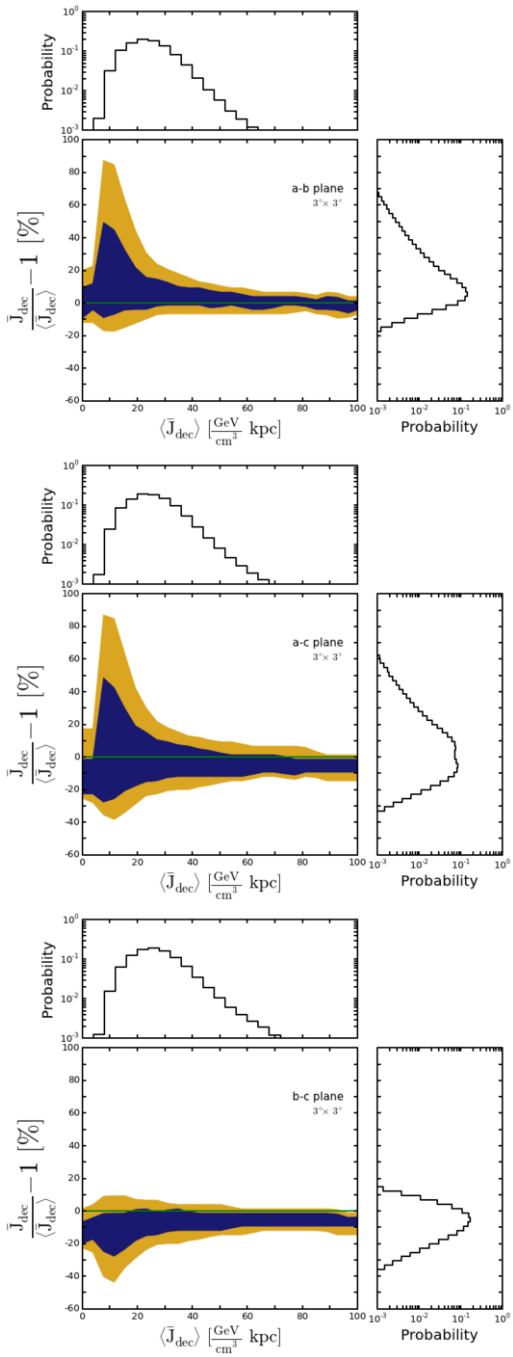

Figure 6: ***Systematic uncertainties on $\bar{J}_{\rm dec}$ for a square ROI of 3° × 3° around the GC for DM decays, due to the non-sphericity of the Milky Way DM halo.*** We show the probability distribution of the deviation of $\bar{J}_{\rm dec}$ from its spherically average value, $\langle\bar{J}_{\rm dec}\rangle$, for the three symmetry planes as a function of $\langle\bar{J}_{\rm dec}\rangle$. The panels and colors of the different contours represent the same as in Fig. 4.

Having performed a statistical analysis of the whole halo sample it is shown that for values of the spherical average of the local DM density of the order of current estimates, i.e., $\langle\rho_\odot\rangle \simeq 0.3 - 0.4$ GeV/cm^3, the actual value of $\rho_\odot$, if the stellar disk coincides with the $a-b$ plane of the DM halo, with a probability of 95%, lies in the interval (see top most panel of Fig. 4)

$$\frac{\rho_\odot}{\langle\rho_\odot\rangle} = 0.83 - 1.35\ . \tag{6}$$

On the other hand, if the stellar disk coincides with the $a-c$ ($b-c$) plane the range, with a probability of 95%, the range is $\rho_\odot/\langle\rho_\odot\rangle = 0.62 - 1.27$ ($0.67 - 1.08$).

Analogously, we have also computed the impact of halo asphericity on the values of the J factors relevant for indirect searches of gamma-rays and neutrinos from DM annihilations and decays at the GC. We note that the variations with respect to the average value depend very weakly on the chosen ROI. However, in these cases the variation with respect to the spherical averages are much smaller than those obtained for the local density. For the case of DM annihilations and $\langle\bar{J}_{\rm ann}\rangle \simeq 590$ (GeV/cm^3)^2 kpc (for a square ROI of $3^\circ \times 3^\circ$ around the GC), the actual value of $\bar{J}_{\rm ann}$, if the stellar disk coincides with the $a-b$ plane of the DM halo, with a probability of 95%, lies in the interval (see upper right panel of Fig. 5)

$$\frac{\bar{J}_{\rm ann}}{\langle\bar{J}_{\rm ann}\rangle} = 0.95 - 1.09\ , \tag{7}$$

whereas it is $\bar{J}_{\rm ann}/\langle\bar{J}_{\rm ann}\rangle = 0.90 - 1.07$ ($0.88 - 1.01$), if the stellar disk coincides with the $a-c$ ($b-c$) plane.

For DM decays and $\langle\bar{J}_{\rm dec}\rangle \simeq 43$ (GeV/cm^3) kpc (for the same ROI), the actual value of $\bar{J}_{\rm dec}$, if the stellar disk coincides with the $a-b$ plane of the DM halo, with a probability of 95%, lies in the interval (see upper right panel of Fig. 6)

$$\frac{\bar{J}_{\rm dec}}{\langle\bar{J}_{\rm dec}\rangle} = 0.93 - 1.13\ , \tag{8}$$

whereas it is $\bar{J}_{\rm dec}/\langle\bar{J}_{\rm dec}\rangle = 0.82 - 1.12$ ($0.83 - 1.04$), if the stellar disk coincides with the $a-c$ ($b-c$) plane.

The ranges above are quoted for values of the spherical averages equal to the J factors for a spherical NFW profile with $r_s = 20$ kpc and $\rho_\odot = 0.3$ GeV/cm^3 at $R_\odot = 8.3$ kpc (for a square ROI of $3^\circ \times 3^\circ$ around the GC), i.e., $\langle\bar{J}_{\rm ann}\rangle \simeq 590$ (GeV/cm^3)^2 kpc and $\langle\bar{J}_{\rm dec}\rangle \simeq 43$ (GeV/cm^3) kpc. However, it turns out that the corresponding values for other spherical DM profiles span a larger range than that owing to halo asphericity. Thus, we conclude that uncertainties originated from the non-sphericity of the Milky Way DM halo are smaller, and thus less important, than the uncertainties coming from the DM density profile.

In summary, we have quantified the systematic uncertainties on the local DM density and the J factors in a statistical way. We note that halo asphericity could imply systematic errors on the local DM density at the level of current uncertainties, but in the case of the J factors they tend to be smaller than other errors. The determination of the DM density profile, not only is important for a better understanding of our galaxy, but also because they represent crucial parameters in direct and indirect DM searches. Hence, assessing their systematic uncertainties, and in particular due to halo asphericity, is of prime importance. Extracting DM properties from a positive signal or from a combination of positive signals will critically depend on the value of these parameters.

References

[1] K. Olive, et al., Chin.Phys. C38 (2014) 090001.
[2] F. Iocco, M. Pato, G. Bertone, Nature 3237. arXiv:1502.03821.
[3] M. Zemp, J. Diemand, M. Kuhlen, P. Madau, B. Moore, et al., Mon.Not.Roy.Astron.Soc. 394 (2009) 641–659. arXiv:0812.2033.
[4] M. Pato, O. Agertz, G. Bertone, B. Moore, R. Teyssier, Phys.Rev. D82 (2010) 023531. arXiv:1006.1322.
[5] A. Klypin, S. Trujillo-Gómez, J. Primack, Astrophys.J. 740 (2011) 102. arXiv:1002.3660.
[6] N. Bernal, J. E. Forero-Romero, R. Garani, S. Palomares-Ruiz, JCAP 1409 (2014) 004. arXiv:1405.6240.
[7] G. Bertone, D. Hooper, J. Silk, Phys.Rept. 405 (2005) 279–390. arXiv:hep-ph/0404175.
[8] L. Bergström, P. Ullio, J. H. Buckley, Astropart.Phys. 9 (1998) 137–162. arXiv:astro-ph/9712318.
[9] K. Riebe, et al., Astronomische Nachrichten (2013) 691–708arXiv:1109.0003.
[10] G. Hinshaw, et al., Astrophys.J.Suppl. 208 (2013) 19. arXiv:1212.5226.
[11] J. F. Navarro, C. S. Frenk, S. D. White, Astrophys.J. 462 (1996) 563–575. arXiv:astro-ph/9508025.
[12] J. F. Navarro, C. S. Frenk, S. D. White, Astrophys.J. 490 (1997) 493–508. arXiv:astro-ph/9611107.
[13] A. Knebe, V. Wiessner, Publ.Astron.Soc.Austral. 23 (2006) 125–128. arXiv:astro-ph/0609361.
[14] X. Xue, et al., Astrophys.J. 684 (2008) 1143–1158. arXiv:0801.1232.
[15] J. Bovy, H.-W. Rix, Astrophys.J. 779 (2013) 115. arXiv:1309.0809.
[16] J. Einasto, Trudy Inst. Astrofiz. Alma-Ata 51 (1965) 87.
[17] A. Burkert, IAU Symp. 171 (1996) 175. arXiv:astro-ph/9504041.